JOURNAL OF AIRCRAFT
Vol. 46, No. 1, January–February 2009

Analytic Drag Prediction for Cambered Wings with Partial Leading-Edge Suction

Lance W. Traub*
Embry-Riddle Aeronautical University, Prescott, Arizona 86301

DOI: 10.2514/1.38558

Rapid estimation of a wing's drag polar accounting for the combined effects of planform and profile drag represents a significant challenge, but is of necessity for preliminary analysis and design. In this paper, methodology is presented culminating in simple expressions allowing the combination of these drag components. Information required is knowledge of the wing's sectional characteristics as well as the planform's lift-curve slope and inviscid span efficiency factor. Airfoil profile drag is interpreted as a loss of leading-edge suction. Effects of camber are explicitly accounted for. The method also lends itself to be used as a design tool in which camber and suction may be optimized to minimize drag, depending on the operating conditions. Comparisons of the method with the experimental data show encouraging agreement.

Nomenclature

AR	=	aspect ratio
C_A	=	finite wing axial-force coefficient
C_D	=	finite wing drag coefficient
C_{DL}	=	finite wing lift-dependent drag coefficient
C_{Dmin}	=	finite wing minimum drag coefficient
C_{Do}	=	finite wing zero-lift drag coefficient
C_L	=	finite wing lift coefficient
C_{Lmd}	=	finite wing lift coefficient at minimum drag
$C_{L\alpha}$	=	finite wing lift-curve slope
C_a	=	sectional axial-force coefficient
C_d	=	sectional drag coefficient
C_{dl}	=	sectional lift-dependent drag coefficient
C_{dmin}	=	sectional minimum drag coefficient
C_l	=	sectional lift coefficient
$C_{l\alpha}$	=	sectional lift-curve slope
$C_{\mathrm{lc.o}}$	=	crossover lift coefficient
C_{lmd}	=	sectional lift coefficient at minimum drag
C_n	=	sectional normal-force coefficient
C_s	=	sectional leading-edge suction coefficient
e	=	Oswald or span efficiency factor
e_i	=	inviscid Oswald or span efficiency factor
e_{p+i}	=	viscous Oswald or span efficiency factor (includes sectional pressure and finite wing drag)
k_i	=	induced or vortex drag parameter
k_p	=	pressure-drag parameter, slope of linearized sectional drag polar
k_{p+i}	=	lift-dependent drag parameter, slope of linearized wing drag polar
α	=	angle of attack
α_{ZL}	=	zero-lift angle of attack
η	=	attainable leading-edge suction parameter
λ	=	taper ratio

Introduction

ACCURATE and economical estimates of the variation of drag coefficient with lift coefficient, the drag polar, are vital for aircraft conceptual and preliminary design studies. Such estimates are also necessary in a research environment for approximation and experimental validation. Rapid estimates of inviscid planform drag (so-called vortex or induced drag) can be made reliably using lifting-line theory, vortex-lattice, or panel methods, depending on the planform under study [1]. Additionally, sectional viscous drag (profile drag) may be estimated with reasonable accuracy using freely available computational tools such as Xfoil.[†] However, incorporation of the sectional profile drag into the total wing drag can be problematic. Frequently, drag comparisons using theoretical computation of the vortex drag in conjunction with use of the experimental zero-lift drag-coefficient yield drag estimates that are always too low compared with the experiment, due to the lack of modeling of the wing profile's pressure drag.

The sectional profile drag is typically decomposed into two components: a skin-friction component due to shear and a pressure-drag component due to flow separation as well as alteration of the effective airfoil shape by the boundary-layer displacement thickness. The skin-friction component is generally assumed to be constant, although it does show a weak variation with lift coefficient. The pressure-drag component typically has a parabolic lift-coefficient dependency. Airfoils that exhibit a drag bucket are designed to have a lift-coefficient range over which extensive laminar flow is maintained; this enables the maintenance of thin boundary layers with a small displacement thickness. Consequently, the resultant pressure distribution is close to the inviscid case, limiting the pressure-drag rise within the bucket region. The variation of pressure drag may be interpreted as a loss of leading-edge suction (as the streamwise forward-acting axial-force and rearward normal-force components no longer exactly cancel). An analysis based on such an approach (wing leading-edge suction) has the benefit of allowing performance estimates for wings with partial or zero leading-edge suction (i.e., sharp leading edges).

Methods to combine sectional and planform drag exist (see [2]), although the approach is numerical. A study by DeLaurier [3] on drag-coefficient estimation for wings with partial leading-edge suction provided a simple expression to estimate the drag of finite wings with camber and partial suction. However, camber contributions were accounted for using the assumption of a circular-arc section in conjunction with the vorticity distribution solution of Schlichting and Truckenbrodt as described in [3]. The method also provided no insight into how to estimate the attainable leading-edge suction or viscous wing efficiency. A significant benefit of the approach was its ability to aid in the design of wings for low-Reynolds-number operation, in which sharp leading edges are often

Received 15 May 2008; revision received 21 July 2008; accepted for publication 22 July 2008.

*Associate Professor, Aerospace and Mechanical Engineering Department. Member AIAA.

[†]Data available online at http://web.mit.edu/drela/Public/web/xfoil/ [retrieved 12 May 2008].

employed to promote transition, with the concomitant penalty of suction loss mitigated by the avoidance of laminar separation.

A simple method to combine both sectional and planform drag coefficients for incompressible untwisted finite wings using an explicit analytic equation set would be of use for all forms of preliminary design. In addition, such a method would be a valuable design tool for estimating the effects of camber and airfoil sections on the total wing drag. In this paper, a method is developed to combine profile and planform drag with explicit treatment of the effects of camber. Relations presented allow both drag estimates as well as that of wing efficiency. Comparisons of the method with the experimental data are presented.

Theoretical Development

In the following sections, drag-coefficient relations incorporating the effect of partial leading-edge suction as well as camber will be developed for airfoils as well as wings. In the derivation, expressions are developed to allow identification of the axial-force constituents: that is, leading-edge suction and camber thrust. Following [3], viscous flow effects are then applied to the identified leading-edge suction term.

Two-Dimensional Airfoils

Development of a sectional relation for the drag coefficient of an airfoil with partial leading-edge suction and camber can be obtained by consideration of the normal and axial forces acting on the profile. Using small-angle approximations of $\sin(\alpha) \approx \alpha$ and $\cos(\alpha) \approx 1$ yields

$$C_{\mathrm{dl}} = C_n \sin(\alpha) - C_a \cos(\alpha) \simeq C_n\alpha - C_a \tag{1}$$

In addition, it may be assumed that $C_n \approx C_l$. The effect of camber may be interpreted as shifting the zero-lift angle of attack,

$$C_n = C_{l\alpha}(\alpha - \alpha_{\mathrm{ZL}})$$

which, with the assumption of a two-dimensional lift-curve slope of 2π/rad, gives

$$C_n = 2\pi(\alpha - \alpha_{\mathrm{ZL}}) \tag{2}$$

For inviscid incompressible flow, $C_d = 0$. Thus, substituting Eq. (2) into Eq. (1) yields

$$C_a = 2\pi(\alpha^2 - \alpha\alpha_{\mathrm{ZL}}) = 2\pi\alpha^2 - 2\pi\alpha\alpha_{\mathrm{ZL}} \tag{3}$$

For a symmetrical profile, $\alpha_{\mathrm{ZL}} = 0$, yielding the well-known expression for the leading-edge suction: $C_s = 2\pi\alpha^2$. Consequently, the two terms on the right-hand side of Eq. (3) are identified, respectively, as the leading-edge suction and the thrust associated with camber. The effects of partial leading-edge suction are frequently incorporated using a parameter η, the attainable suction [4,5], which varies from 1 (full suction) to 0 (no suction). A study by Carlson and Mack [6] indicated that the suction level attained is dependent on the airfoil's leading-edge radius, Reynolds number, limiting pressure coefficient, Mach number normal to the leading edge, and the airfoil's thickness-to-chord ratio.

Incorporation of this parameter into Eq. (3) yields

$$C_a = \eta 2\pi\alpha^2 - 2\pi\alpha\alpha_{\mathrm{ZL}} \tag{4}$$

Equation (4) suggests that camber does not affect the leading-edge suction developed at a given α. Substitution of Eqs. (2) and (4) into Eq. (1) gives

$$C_{\mathrm{dl}} = 2\pi(1 - \eta)\alpha^2 \tag{5}$$

A similar relation was derived in [3] in a different fashion. What is significant is that Eq. (5) clearly shows that camber does not contribute to drag for an airfoil at a given angle of attack. The extra axial force associated with camber ($-2\pi\alpha\alpha_{\mathrm{ZL}}$) exactly counteracts the additional rearward component of the lift (or normal force) due to camber, yielding no net change in the drag coefficient. Based on an equal lift-coefficient comparison, a different result is determined. From Eq. (2), the required airfoil angle of attack for a desired C_l is

$$\alpha = \frac{C_l}{2\pi} + \alpha_{\mathrm{ZL}} \tag{6}$$

Substitution of Eq. (6) into Eq. (5) shows

$$C_{\mathrm{dl}} = 2\pi(1 - \eta)\left(\frac{C_l}{2\pi} + \alpha_{\mathrm{ZL}}\right)^2 \tag{7}$$

The relation shows that for an airfoil with partial or zero leading-edge suction ($0 \le \eta < 1$), increasing α_{ZL} reduces C_d for a given C_l (α_{ZL} is negative). Equation (7) indicates a parabolic dependency of the drag coefficient with a drag-coefficient minimum for $C_l > 0$. Consequently, comparison of a symmetrical and cambered wing with equal attainable suction (same η) shows a crossover above which the cambered airfoil will always have lower drag (for $\eta < 1$). This is shown explicitly in Fig. 1, with η arbitrarily selected as 0.8. The crossover point is established using Eq. (7). At the crossover, the two airfoils will have equal C_d; hence, we may write

$$2\pi(1 - \eta)\left(\frac{C_{\mathrm{lc.o}}}{2\pi} + \alpha_{\mathrm{ZL}}\right)^2 = 2\pi(1 - \eta)\left(\frac{C_{\mathrm{lc.o}}}{2\pi}\right)^2$$

which, upon solving for the crossover lift coefficient, yields

$$C_{\mathrm{lc.o}} = -\pi\alpha_{\mathrm{ZL}} \tag{8}$$

This lift coefficient corresponds to an angle of attack of $\alpha_{\mathrm{ZL}}/2$ for the cambered airfoil and $-\alpha_{\mathrm{ZL}}/2$ for the symmetrical airfoil, as shown by Eq. (6) and as evident in Fig. 1. Thus, for all lift coefficients greater than $C_{\mathrm{lc.o}}$, a cambered airfoil will show a lower drag coefficient than a symmetrical profile with equal attainable suction. Equation (7) reveals that reductions in drag due to camber are a result of the decrease in the required incidence to generate a given lift coefficient. For lift coefficients less than $C_{\mathrm{lc.o}}$, the cambered airfoil is at a greater negative angle of attack than the symmetrical profile is at a positive incidence to generate the same C_l (see Fig. 1). The minimum drag coefficient for the cambered profile is given when $C_l = -2\pi\alpha_{\mathrm{ZL}}$ and corresponds to the airfoil at a 0 deg geometric angle of attack. This lift coefficient also corresponds to the value

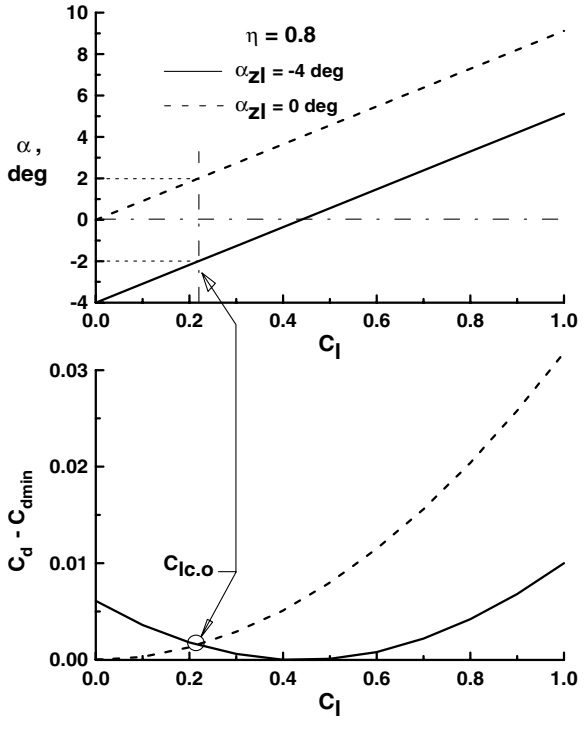

Fig. 1 Effect of camber on the theoretical drag polar.

beyond which the axial force changes from a drag to a thrust. Note, however, that camber does, in general, increase the minimum drag coefficient compared with a symmetrical profiled section. Modeling of airfoil design features such as a drag bucket using Eq. (7) would be effected through η; that is, in the bucket region, the attainable thrust would be approximately 100% so that the drag increment above that of skin friction would be negligible.

Three-Dimensional Wings

The drag polar for a symmetrical untwisted finite wing is often written as

$$C_D = C_{Do} + k_{p+i}C_L^2 \tag{9}$$

The first term on the right-hand side is the drag coefficient at zero lift and is usually attributed to skin-friction drag, although a small pressure-drag component may also be present. The second term represents the contribution of both sectional-pressure- and planform-dependent induced (or vortex) drag ($k_{p+i}C_L^2$). For wings, both the pressure component of the profile drag coefficient ($k_pC_L^2$) and the planform-dependent induced drag coefficient ($k_iC_L^2$) vary with the square of the lift coefficient. When estimating the drag polar of a wing using an inviscid theoretical approach such as numerical lifting-line theory or a vortex-lattice-type code, airfoil-profile effects due to viscosity are naturally not accounted for, although effects of twist may be modeled. The drag due to lift that is calculated is associated with the planform of the wing (i.e., vortex or induced drag). Profile effects may be incorporated using the following expression [7] for wings with a cambered or symmetrical section:

$$C_D = C_{\text{dmin}} + k_p(C_L - C_{\text{lmd}})^2 + k_iC_L^2 \tag{10}$$

where C_{dmin} is the minimum airfoil drag coefficient, C_{lmd} is the lift coefficient at which minimum drag occurs for the airfoil, and k_p is determined from airfoil data (it is the slope of the linearized drag polar). The use of Eq. (10) requires only 2-D sectional data and a 3-D estimate of vortex drag (k_i). However, this relation generally fails for airfoil profiles that may exhibit "poorly behaved" polars or those with a drag bucket. Consequently, an expression that would be better suited to cope with arbitrary airfoil polars and allow a discrete treatment of camber effects (implemented though the zero-lift angle) would be valuable. To this end, relations for the finite wing case may be developed in a similar fashion to that presented for airfoils. Note that the development is concerned with lift-dependent drag and excludes skin-friction drag in the formal derivation; it can simply be added to the final drag due to lift approximation.

Writing the axial force as (assuming small-angle approximations)

$$C_A = C_L\alpha - C_{\text{DL}} \tag{11}$$

and noting that for a cambered wing, we may write

$$C_L = C_{L\alpha}(\alpha - \alpha_{\text{ZL}}) \tag{12}$$

approximating the planform's lift-dependent drag coefficient as

$$C_{\text{DL}} = \frac{C_L^2}{\pi \text{AR} e_i} \tag{13}$$

where e_i is the Oswald efficiency factor associated with planform efficiency effects and may be considered to be an inviscid spanwise efficiency factor. Substituting Eqs. (12) and (13) into Eq. (11) results in

$$C_A = C_{L\alpha}(\alpha - \alpha_{\text{ZL}})\alpha - \frac{C_{L\alpha}^2(\alpha - \alpha_{\text{ZL}})^2}{\pi \text{AR} e_i} \tag{14}$$

Multiplying Eq. (14) and collecting terms gives

$$C_A = C_{L\alpha}\alpha^2 - \frac{C_{L\alpha}^2\alpha^2}{\pi \text{AR} e_i} - C_{L\alpha}\alpha\alpha_{\text{ZL}} + \frac{C_{L\alpha}^2(2\alpha\alpha_{\text{ZL}} - \alpha_{\text{ZL}}^2)}{\pi \text{AR} e_i} \tag{15}$$

where the first two terms on the right-hand side may be interpreted as those due to leading-edge suction, and the third and forth terms are attributed to camber thrust. The pressure-drag coefficient of the wing's section is considered as causing a loss of leading-edge suction (or a diminished net axial force). As implemented in the previous airfoil development, an attainable thrust parameter η with values ranging from 0 to 1 will be used. Full suction, and hence zero profile pressure drag, would correspond to $\eta = 1$, and $\eta = 0$ would indicate an airfoil with a sharp leading-edge such that no suction is developed:

$$C_A = \eta\left(C_{L\alpha} - \frac{C_{L\alpha}^2}{\pi \text{AR} e_i}\right)\alpha^2 - C_{L\alpha}\alpha\alpha_{\text{ZL}} + \frac{C_{L\alpha}^2(2\alpha\alpha_{\text{ZL}} - \alpha_{\text{ZL}}^2)}{\pi \text{AR} e_i} \tag{16}$$

The lift-dependent drag coefficient is simply estimated using

$$C_{\text{DL}} = C_L\alpha - C_A \tag{17}$$

Substituting Eqs. (12) and (16) into Eq. (17) results in

$$C_{\text{DL}} = (1 - \eta)C_{L\alpha}\alpha^2 + \frac{C_{L\alpha}^2}{\pi \text{AR} e_i}(\eta\alpha^2 - 2\alpha\alpha_{\text{ZL}} + \alpha_{\text{ZL}}^2) \tag{18}$$

Equation (18) allows estimation of the drag coefficient of wings including the effect of the sectional profile drag. The Oswald efficiency factor e_i, and the finite wing lift-curve slope $C_{L\alpha}$ may be estimated using any suitable theoretical or numerical technique. The zero-lift angle of attack is that for the section: α_{ZL}. For cambered profiles, Eq. (18) must be implemented as a function of the lift coefficient. Thus, using

$$\alpha = \frac{C_L}{C_{L\alpha}} + \alpha_{\text{ZL}} \tag{19}$$

in conjunction with Eq. (18) results in the final expression for estimating the lift-dependent drag coefficient of a finite wing:

$$C_{\text{DL}} = (1 - \eta)C_{L\alpha}\left(\frac{C_L}{C_{L\alpha}} + \alpha_{\text{ZL}}\right)^2 + \frac{C_{L\alpha}^2}{\pi \text{AR} e_i}\left[\eta\left(\frac{C_L}{C_{L\alpha}} + \alpha_{\text{ZL}}\right)^2 - 2\left(\frac{C_L}{C_{L\alpha}} + \alpha_{\text{ZL}}\right)\alpha_{\text{ZL}} + \alpha_{\text{ZL}}^2\right] \tag{20}$$

In the instance that the airfoil section attains full suction (i.e., $\eta = 1$), then Eq. (20) simplifies to

$$C_{\text{DL}} = \frac{C_{L\alpha}^2}{\pi \text{AR} e_i} \tag{21}$$

Thus, for a wing with full leading-edge suction, camber has no effect on the lift-dependent drag coefficient. Notice that full suction does not necessarily imply elliptic loading in the context of this analysis, but that the lift-dependent drag is due to planform shape and hence vortex drag only.

An estimate of the attainable suction can be determined from either experimental or theoretical estimates of the airfoil's drag polar. Naturally, it is imperative that the sectional and finite wing test conditions are similar. Mathematically, the attainable suction may be expressed as the actual axial force divided by the maximum axial force; hence,

$$\eta = \frac{C_l\alpha - \Delta C_d}{C_l\alpha} = \frac{C_l\alpha - (C_d - C_{\text{dmin}})}{C_l\alpha} \tag{22}$$

Substitution of Eq. (6) yields

$$\eta = 1 - \frac{(C_d - C_{\text{dmin}})}{C_l[(C_l/C_{l\alpha}) + \alpha_{\text{ZL}}]} \tag{23}$$

Frequently, $C_{l\alpha}$ is assumed to be 2π/rad. Equations (20) and (23) allow estimation of the planform and profile drag for untwisted wings in incompressible flow, if sectional data are known, as well as the planform-efficiency factor and finite wing lift-curve slope. Total C_D may be estimated by adding C_{Dmin} to Eq. (20). Once η has been determined as a function of C_l for the section, η is assumed to have the same average value as a similar finite wing C_L when evaluated in Eq. (20).

It would also be of value to be able to estimate the span or Oswald efficiency factor e for wings including profile effects, such that e estimation would be representative of that seen in experiment or flight. To this end, Eq. (20) may be used, although a slightly more compact expression might result in a more tractable resulting equation.

DeLaurier [3] developed an expression to estimate the drag coefficient of wings with partial leading-edge suction based upon an assumed circular-arc camber distribution. The resulting expression was given as (after modification to the signs for consistency)

$$C_{\mathrm{DL}} = \eta \frac{C_L^2}{\pi \mathrm{AR} e_i} + (1-\eta)\left(\frac{C_L^2}{C_{L\alpha}} + 2\alpha_{\mathrm{ZL}} C_L + 2\pi\alpha_{\mathrm{ZL}}^2\right) \tag{24}$$

The lift-dependent drag coefficient for cambered wings may also be estimated using the following modified form of the drag polar [7]:

$$C_{\mathrm{DL}} = k_{p+i}(C_L - C_{\mathrm{Lmd}})^2 = \frac{(C_L - C_{\mathrm{Lmd}})^2}{\pi \mathrm{AR} e_{p+i}} \tag{25}$$

where profile and planform effects are combined in k_{p+i} and e_{p+i}. Equating Eqs. (24) and (25) results in

$$e_{p+i} = \frac{(C_L - C_{\mathrm{Lmd}})^2}{\eta(C_L^2/e_i) + (1-\eta)\pi \mathrm{AR}[(C_L^2/C_{L\alpha}) + 2\alpha_{\mathrm{ZL}} C_L + 2\pi\alpha_{\mathrm{ZL}}^2]} \tag{26}$$

Equation (26) requires an estimate for the lift coefficient for minimum drag, C_{Lmd}. This may be estimated by differentiating Eq. (24) with respect to C_L. Consequently,

$$\frac{dC_{\mathrm{DL}}}{dC_L} = 0 = 2\eta \frac{C_L}{\pi \mathrm{AR} e_i} + (1-\eta)\left(\frac{2C_L}{C_{L\alpha}} + 2\alpha_{\mathrm{ZL}}\right)$$

Setting $C_L = C_{\mathrm{Lmd}}$ and solving for C_{Lmd} yields

$$C_{\mathrm{Lmd}} = \frac{(\eta-1)\alpha_{\mathrm{ZL}}}{\{(\eta/\pi \mathrm{AR} e_i) + [(1-\eta)/C_{L\alpha}]\}} \tag{27}$$

Substituting Eq. (27) into Eq. (26) results in

$$e_{p+i} = \left(C_L - \frac{(\eta-1)\alpha_{\mathrm{ZL}}}{(\eta/\pi \mathrm{AR} e_i) + [(1-\eta)/C_{L\alpha}]}\right)^2 \Bigg/ \times \left[\eta \frac{C_L^2}{e_i} + (1-\eta)\pi \mathrm{AR}\left(\frac{C_L^2}{C_{L\alpha}} + 2\alpha_{\mathrm{ZL}} C_L + 2\pi\alpha_{\mathrm{ZL}}^2\right)\right] \tag{28}$$

Equation (28) may be used to estimate the effective (viscous) Oswald efficiency factor for wings using knowledge of the sectional drag polar and the finite wing lift-curve slope. In conjunction with Eq. (25), Eq. (28) may be used for drag estimates similar to Eq. (20). It is of interest to explore Eq. (28) for cases of zero leading-edge suction and no camber. Setting $\eta = 0$ results in

$$e_{p+i} = \frac{(C_L + \alpha_{\mathrm{ZL}} C_{L\alpha})^2}{\pi \mathrm{AR}[(C_L^2/C_{L\alpha}) + 2\alpha_{\mathrm{ZL}} C_L + 2\pi\alpha_{\mathrm{ZL}}^2]} \tag{29}$$

Setting $\eta = \eta$ but $\alpha_{\mathrm{ZL}} = 0$ yields

$$e_{p+i} = \frac{1}{(\eta/e_i) + (1-\eta)(\pi \mathrm{AR}/C_{L\alpha})} \tag{30}$$

Setting $\eta = 0$ gives

$$e_{p+i} = \frac{C_{L\alpha}}{\pi \mathrm{AR}} \tag{31}$$

Equation (31) represents the lowest value that the efficiency factor may attain: that is, a flat plate with zero leading-edge suction. Setting $\eta = 1$ in Eq. (30) shows $e_{p+i} = e_i$; hence, there is no profile-pressure-drag constituent and the span efficiency factor is essentially inviscid.

Experimental Validation and Analysis

Sivells [8] presented an experimental investigation into the effects of washout on a $\mathrm{AR} = 9$ wing with 0.4 taper. Tests were undertaken at $Re = 4.4 \times 10^6$. Of particular interest for validation of Eq. (20) is that Sivells also recorded the sectional drag coefficient at the same test conditions using both force balance and wake surveys. Consequently, sectional estimates of the attainable suction are assumed to be representative for the wing. Figure 2 presents the sectional drag polar, the calculated attainable suction parameter, and the linearized polar [required for Eq. (10)]. Suction levels calculated using Eq. (23) are seen to be close to 100% ($\eta = 1$) within the drag bucket, indicating little sectional pressure drag. Estimates of the wing's drag polar are detailed in Fig. 3. Sivells' experimental data are compared with predictions using two equations developed in this paper [Eqs. (20) and (28)] as well as Delaurier's [3] expression and that in [7]. The theoretical full suction (solid gray line) is representative of a drag estimate that may be determined using a numerical method (e.g., a vortex-lattice code) to estimate e_i in conjunction with the experimental value for C_{Dmin}. A significant underprediction of drag is clearly evident due to the exclusion of the profile's pressure-drag constituent. As shown, all three methods using the variable attainable suction concept show excellent accord with the experiment. The estimate using Eq. (20) appears to show the most encouraging agreement. The nonparabolic form of the sectional polar is clearly reflected in the poorer predictive capability of Eq. (10).

The linearized drag polar corresponding to the data in Fig. 3 is displayed in Fig. 4. The slope of this polar was used to estimate the wing's efficiency factor e_{p+i}, which includes both sectional and planform contributions. Also included in the upper inset plot is an estimate of the wing's efficiency using Eq. (28). The estimate clearly shows that the wing's efficiency is not a constant, but shows a significant reduction in the initial drag-rise region of the polar ($C_L \approx 0.37$) (see Fig. 2).

Figure 5 explores the theoretical effect of camber and attainable suction on the test wing of [8]. The predictions indicate that camber

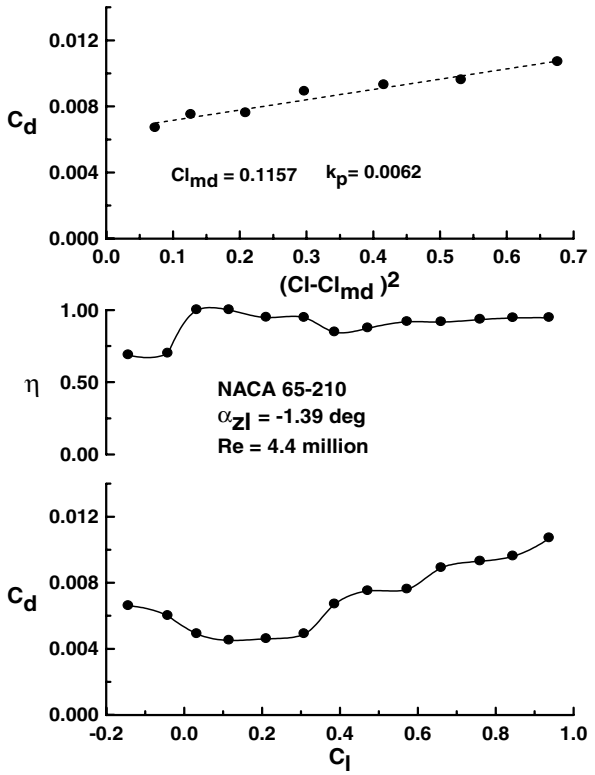

Fig. 2 Experimental sectional characteristics for NACA 65-210 (top to bottom: linearized drag polar, attainable leading-edge suction, and drag polar); data from [8].

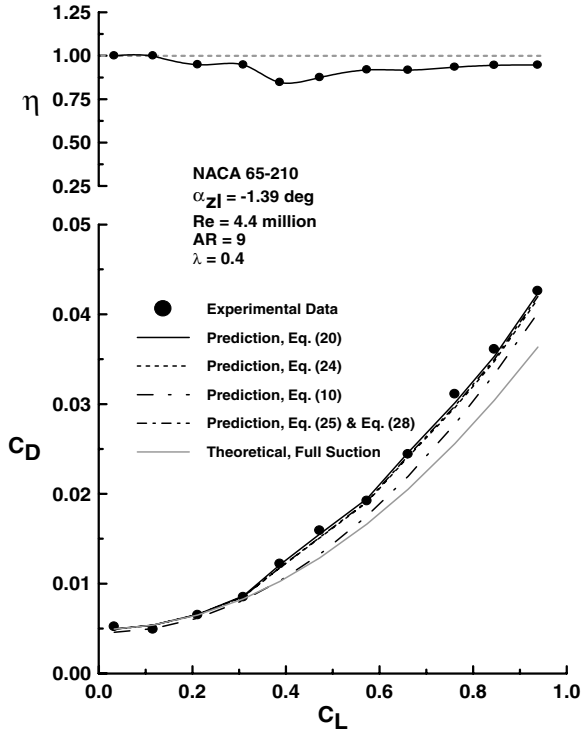

Fig. 3 Comparison of theory and experimental attainable leading-edge suction and drag polar for tapered NACA 65-210 sectioned wing; data from [8].

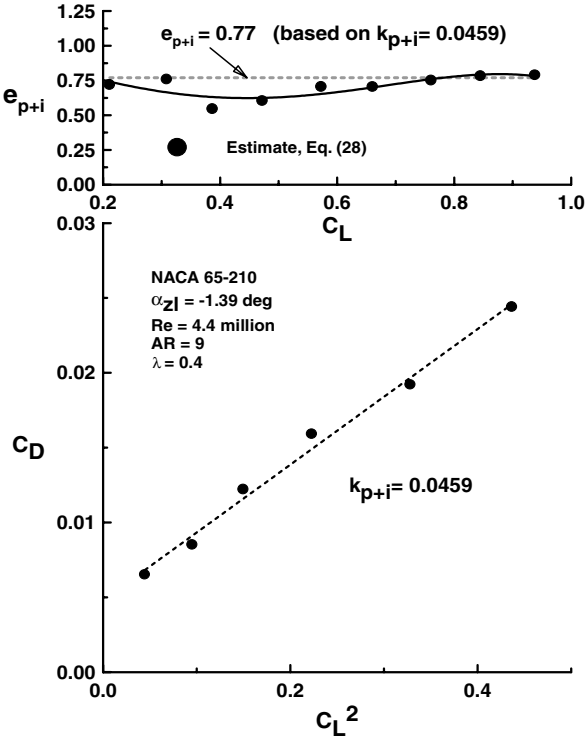

Fig. 4 Comparison of theoretical and experimental wing efficiency for tapered NACA 65-210 sectioned wing; data from [8].

has a far more significant effect in reducing drag when leading-edge suction levels are low. As the attained suction tends toward 100%, camber's effect diminishes to zero. As mentioned previously, camber reduces drag for a given lift coefficient by reducing the required geometric angle of attack of the wing. For a wing with a sharp leading edge (as may be used at low Reynolds numbers), the attainable suction is zero. However, camber may be used to achieve

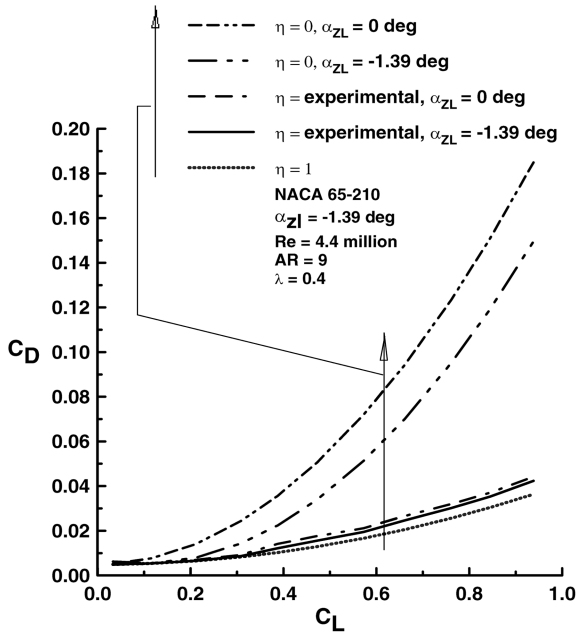

Fig. 5 Theoretical drag polar indicating the effect of attainable suction level and camber.

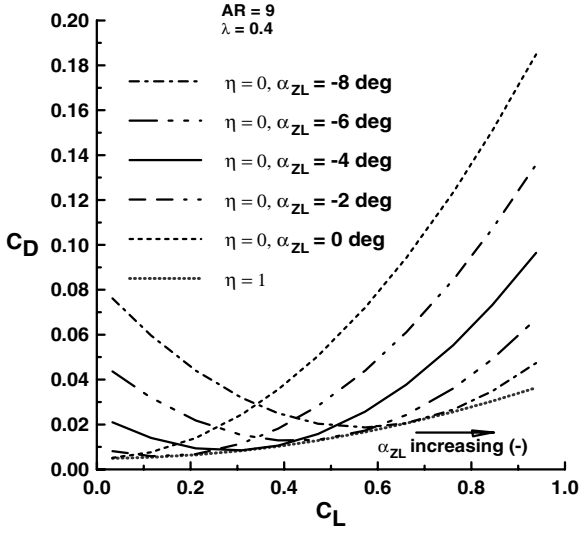

Fig. 6 Theoretical drag polar indicating the effect of camber for a wing with zero leading-edge suction.

drag coefficients comparable with those with full suction over a moderate C_L range; this is explored explicitly in Fig. 6. As may be seen, increasing the zero-lift angle of attack (effect of camber) moves the minimum-drag-coefficient region to higher $C_L s$, a well-known effect of camber. At higher loading conditions $C_L > 0.6$, significant camber (large α_{ZL}) is required to minimize drag. Figure 6 clearly indicates that for operation of a sharp-edged profile, a wing with variable camber (potential morphing application) would be necessary to achieve efficient flight operation over a significant extent of the flight envelope.

Figures 7 and 8 present experimental data reported by Anderson [9]. Results are displayed for the sectional data of a NACA 4412 at $Re = 8.26 \times 10^6$. Also shown is the linearized drag polar (upper inset) for determination of the pressure drag due to lift parameter k_p. The NACA 4412 section was used in an $AR = 6$ elliptic planform wing, experimental data for which are displayed in Fig. 8. Agreement of all methods with the experimental data is seen to be very good, with Eq. (20) showing the closest accord. The equation of DeLaurier [3] [Eq. (24)], although showing generally good agreement with the

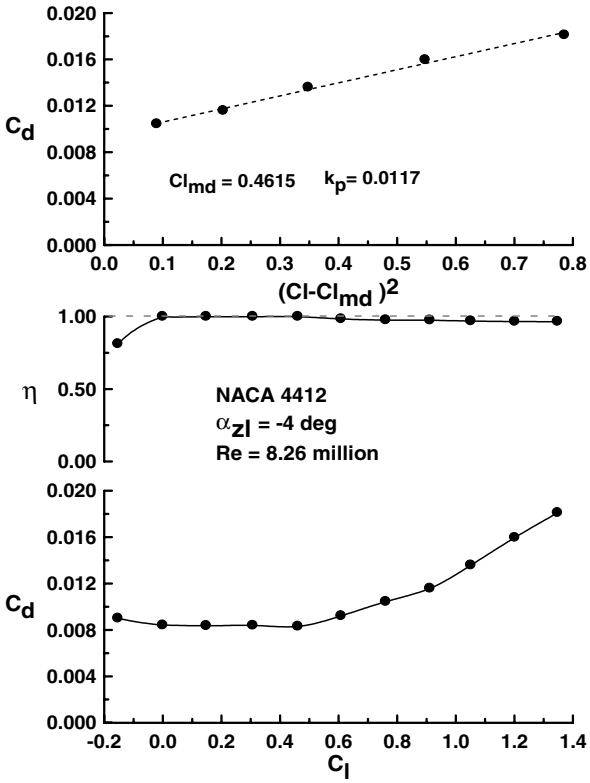

Fig. 7 Experimental sectional characteristics for NACA 4412 (top to bottom: linearized drag polar, attainable leading-edge suction and drag polar); data from [9].

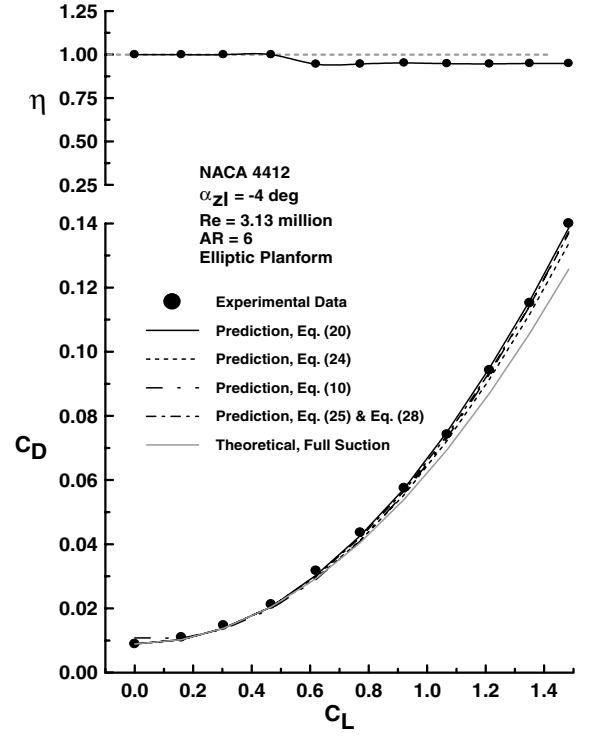

Fig. 8 Comparison of theory and experimental attainable leading-edge suction and drag polar for elliptic NACA 4412 sectioned wing; data from [9].

experiment overall, shows the poorest agreement with the other theoretical methods presented. In all instances, agreement with the experiment is greatly improved by incorporation of the profile drag (i.e., compared with the full-suction line). Notice that Eq. (10) provides better agreement with the experiment than that shown in Fig. 6. This is as a result of the sectional polar's closer accord with a parabolic fit; hence, the value of k_p used in Eq. (10) is a better representation.

Figure 9 shows the linearized drag polar for the wing as well as estimates of the wing's efficiency using Eq. (28). As may be seen, the theoretical prediction of e_{p+i} is in good agreement with the experiment. Figure 10 presents the theoretical effect of attainable suction and camber on the drag coefficient. As observed in Fig. 5, the beneficial effects of camber are most pronounced when attainable suction levels are low. Effects of camber for this planform with zero

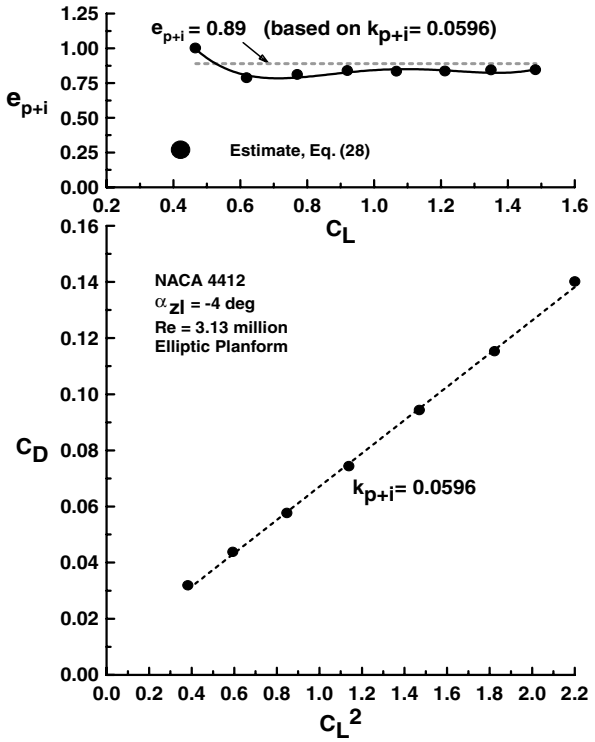

Fig. 9 Comparison of theoretical and experimental wing efficiency for elliptic NACA 4412 sectioned wing; data from [9].

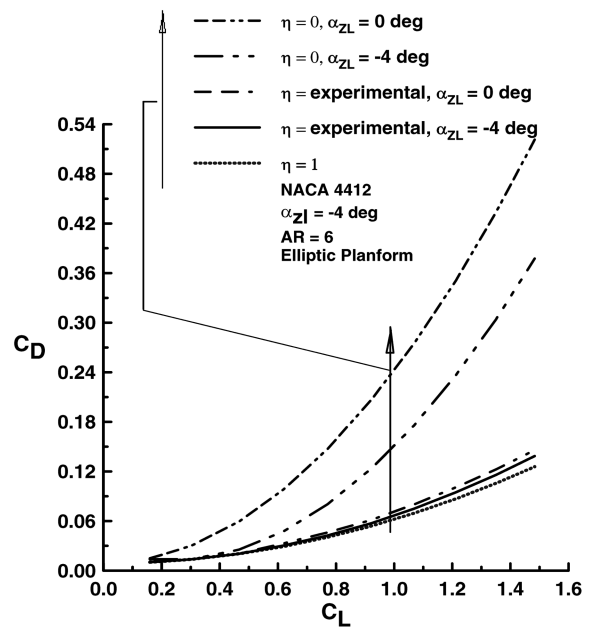

Fig. 10 Theoretical drag polar indicating the effect of attainable suction level and camber.

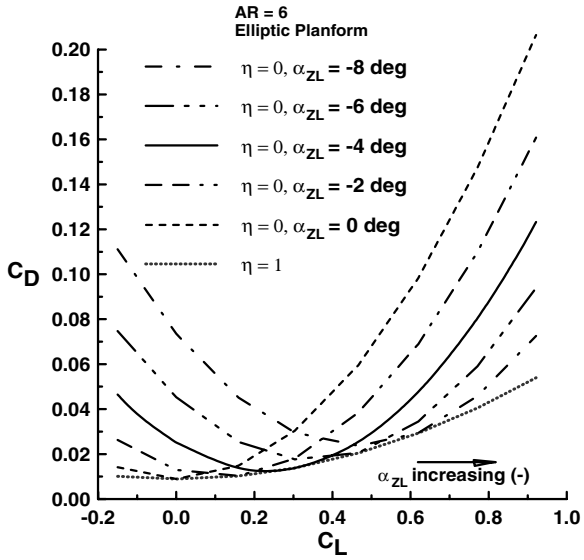

Fig. 11 Theoretical drag polar indicating the effect of camber for a wing with zero leading-edge suction.

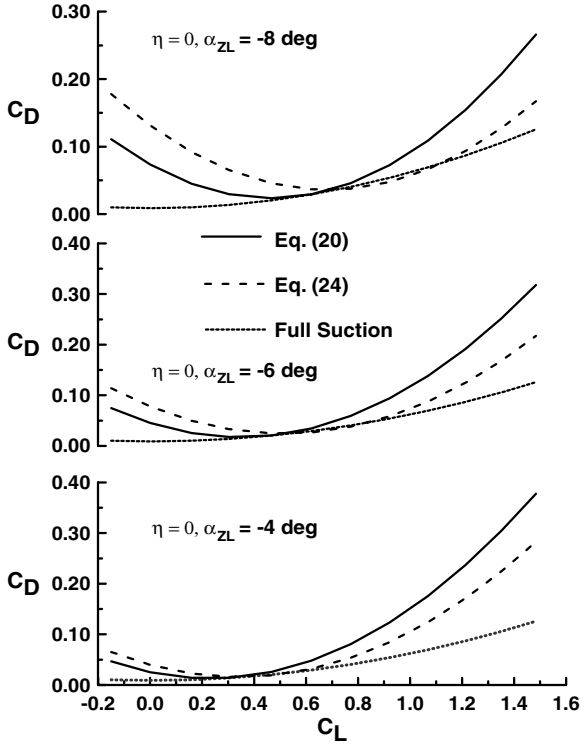

Fig. 12 Theoretical estimates comparing Eqs. (20) and (24) to indicate the effect of camber for an AR = 6 elliptic planform wing with zero leading-edge suction.

leading-edge suction are investigated in Fig. 11. Increasing camber is seen as a necessity for efficient lift production at higher C_L. A comparison with $\eta = 0$, as may be seen for low-Reynolds-number cambered-plate airfoils (assuming the AR = 6 elliptic wing as the base planform) of the present method [Eq. (20)] with DeLaurier's [3] equation (24), is displayed in Fig. 12. As may be seen, the agreement between the two theoretical expressions is poor for the three displayed cases. Numerical evaluation shows improving agreement between the equations with increasing attainable suction η. However, it may be seen that Eq. (24) predicts drag coefficients below that with full suction as α_{ZL} increases. This is not a physical reality and may be an issue with the underlying assumptions in the derivation of Eq. (24). As mentioned in [3], Eq. (24) may have

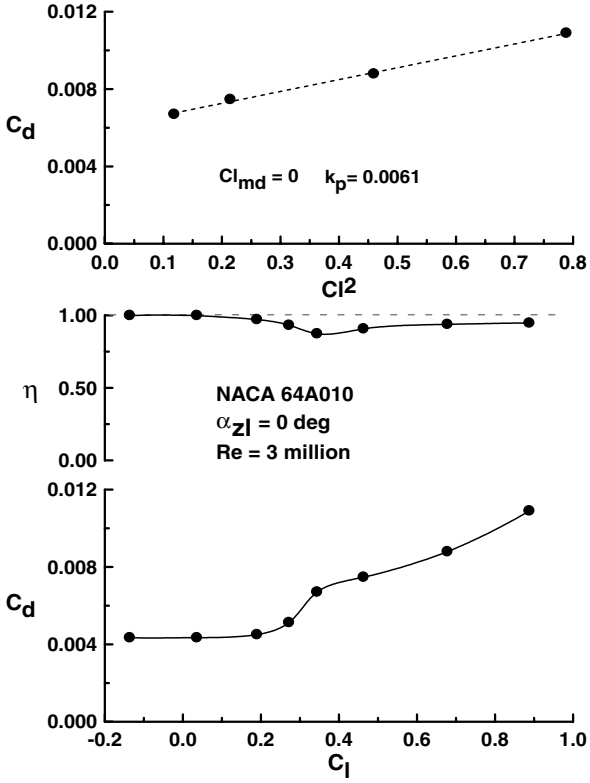

Fig. 13 Experimental sectional characteristics for NACA 64A010 (top to bottom: linearized drag polar, attainable leading-edge suction, and drag polar); data from [11].

limited applicability for airfoil profiles that are not circular arcs. Nonetheless, the results in this study indicate that Eq. (24), although not showing the same level of predictive accuracy as Eq. (20), still provides good estimates and is a slightly simpler expression.

Johnson and Hagerman [10] investigated the effect of flaps on a rectangular-reflection-plane model of AR = 3.13 at $Re = 4.5 \times 10^6$. However, their data did not include a sectional drag polar. Consequently, to compare with their results, the drag polar of the profile, a NACA 61A010, was estimated from data in [11]. The sectional polar is shown in Fig. 13. The data were acquired at $Re = 3 \times 10^6$. The wing experimental drag polar and theoretical predictions are shown in Fig. 14. Equation (20) is seen to underpredict the drag coefficient, although the estimate is better than

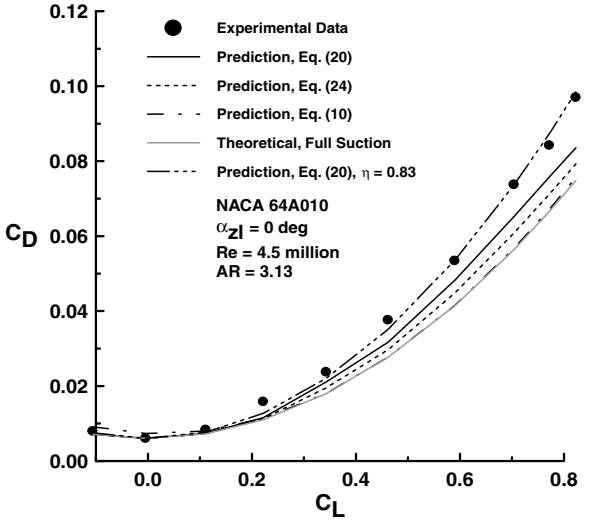

Fig. 14 Comparison of theory and experimental drag polar for a rectangular NACA 64A010 sectioned wing; data from [10].

with Eq. (24) or Eq. (10). Setting $\eta = 0.83$ shows good agreement with the experiment. The data in the plot clearly show the importance of using sectional-drag-polar data that are representative of that of the wing being approximated. Nonetheless, incorporation of the profile pressure drag (even if not totally representative) still yields a better drag-coefficient estimate than that based purely on vortex drag.

If sectional data are not available for the airfoil profile, the attainable suction may be estimated using either the method of Carlson and Mack [6] or the method of Kulfan [12]. The method of Kulfan assumes that the attainable suction starts to reduce below 100% when the airfoil's leading-edge suction exceeds the leading-edge drag (a geometric property of the airfoil's leading-edge radius). The method of Carlson and Mack [6] accounts for the effect of numerous parameters on the attainable suction and combines them into a curve-fit-type function.

Conclusions

In this paper, expressions are developed allowing the combination of a wing's sectional and planform drag to yield estimates of the total lift-dependent drag coefficient. The method is applicable in incompressible flow for untwisted wings. The formulation treats sectional pressure drag as a loss of leading-edge suction. The attainable leading-edge suction is estimated from airfoil sectional data and, in combination with the calculated wing-vortex drag, yields a total lift-dependent-drag estimate. An equation is also presented allowing an estimate of the wing's spanwise efficiency factor, incorporating both sectional and planform effects. The method also lends itself to be used as a design tool in which camber and suction may be optimized to minimize drag, depending on the operating conditions. Comparisons of the resulting equations with the experimental data show encouraging agreement.

References

[1] Katz, J., and Plotkin, A., *Low-Speed Aerodynamics From Wing Theory to Panel Methods*, McGraw–Hill, New York, 1991, Chaps. 8, 12.

[2] Sivells, J. C., and Neely, R. H., "Method for Calculating Wing Characteristics by Lifting-Line Theory Using Nonlinear Section Data," NACA TN 865, Langley, VA, Dec. 1946.

[3] DeLaurier, J., "Drag of Wings with Cambered Airfoils and Partial Leading-Edge Suction," *Journal of Aircraft*, Vol. 20, No. 10, 1983, pp. 882–886.
doi:10.2514/3.44959

[4] Traub, L. W., "Analytic Prediction of Lift for Delta Wings with Partial Leading-Edge Thrust," *Journal of Aircraft*, Vol. 31, No. 6, 1994, pp. 1426–1429.
doi:10.2514/3.46672

[5] Carlson, H. W., and Mack, R. J., "Studies of Leading-Edge Thrust Phenomena," *Journal of Aircraft*, Vol. 17, No. 12, 1980, pp. 890–897.
doi:10.2514/3.57981

[6] Carlson, H. W., and Mack, R. J., "Estimation of Attainable Leading-Edge Thrust for Wings at Subsonic and Supersonic Speeds," NASA Langley Research Center TP 1500, Hampton VA, 1979.

[7] Traub, L. W., "Unified Approximation for Nonparabolic Drag Polars," *Journal of Aircraft*, Vol. 44, No. 1, 2007, pp. 343–346.
doi:10.2514/1.28646

[8] Sivells, J. C., "Experimental and Calculated Characteristics of Three Wings of NACA 64-210 and 65-210 Airfoil Sections with and Without Washout," NACA TN 1422, Aug. 1947.

[9] Anderson, R. F., "The Experimental and Calculated Characteristics of 22 Tapered Wings," NACA Rept. 627, Nov. 1937.

[10] Johnson, H. S., and Hagerman, J. R., "Wind-Tunnel Investigation at Low Speed of an Unswept Untapered Semispan Wing of Aspect Ratio 3.13 Equipped with Various 25-Percent-Chord Flaps," NACA TN 2080, Apr. 1950.

[11] Abbott, I. H., and von Doenhoff, A. E., *Theory of Wing Sections*, Dover, New York, 1959, p. 595.

[12] Kulfan, R. M., "Wing Geometry Effects on Leading Edge Vortices," AIAA Paper 79-1872, Aug. 1979.